Energy Storage Materials 71 (2024) 103679

Contents lists available at ScienceDirect

Energy Storage Materials

journal homepage: www.elsevier.com/locate/ensm

Fluorine-based localization effect for stabilized high-voltage magnesium phenolic electrolyte

Pei Liu [a], Juncai Long [a], Rui Wang [a], Yuhao Zhou [a], Baihua Qu [c], Lei Zhang [a,b,*], Xiaoyuan Zhou [c,*], Qinyou An [a,b,*]

[a] State Key Laboratory of Advanced Technology for Materials Synthesis and Processing, Wuhan University of Technology, Wuhan 430070, China
[b] Hubei Longzhong Laboratory, Wuhan University of Technology (Xiangyang Demonstration Zone), Xiangyang 441000, China
[c] National Engineering Research Center for Magnesium Alloys, Chongqing University, Chongqing 400044, China

ARTICLE INFO

Keywords:
Mg metal batteries
Electrolytes
Fluorine-based localization effect
Solid electrolyte interface
Oxidation stability

ABSTRACT

The design of electrolytes with excellent compatibility and high oxidation stability has long been the prerequisite for realizing high-voltage rechargeable magnesium batteries (RMBs). Compared with other chlorine-containing electrolytes, phenol-based magnesium electrolytes possess better water-oxygen resistance, simpler synthesis steps, and lower ingredient costs making it very promising for applications. However, lower oxidation stability renders it difficult to be applied in high-voltage RMBs. Herein, for the first time, we propose to utilize the fluorine-based localization effect (fluorine substitution from 2,4 o-para site on phenol enhances electrolyte oxidation stability) to design M24AT electrolyte (2,4-F_2PhOMgCl + $AlCl_3$ / THF). As-prepared M24AT electrolyte exhibits superior oxidation stability (3.9 V vs. Mg/Mg^{2+}) than any other phenol-based electrolyte. Additionally, it in-situ generates a fluorinated solid electrolyte interface (SEI) that stabilizes the Mg anode during cycling. Consequently, the Mg||Mo_6S_8 cells with M24AT electrolyte demonstrate ~100 % capacity retention after 500 cycles at 1C. Besides, the high-voltage stability of the M24AT electrolyte is displayed by electrochemical testing with Mg||PAQI full cells, which operate at voltages up to 3.0 V and exhibit greater than 300 stable cycles at 200 mA g^{-1}, with average coulombic efficiency (CE) of ~98 %. The proposed design strategy of fluorine-based localization facilitates the application of phenol-based electrolytes in high-voltage RMBs.

1. Introduction

The current energy density of lithium-ion batteries is nearing the theoretical upper bound [1,2]. Furthermore, the development of lithium metal batteries has also been limited by the scarcity of lithium metal and the safety problems caused by the dendrite formation on the lithium anode [3–5]. However, the use of Mg metal directly as an anode for RMBs has specific advantages: (1) Mg anode is not prone to the formation of magnesium dendrites, providing a high level of safety. (2) Mg metal has a low electric potential (−2.37 V vs. SHE). (3) Mg metal anode demonstrates high theoretical mass specific capacity (2205 mAh g^{-1}) and volumetric specific capacity (3833 mAh cm^{-3}) [6,7]. Therefore, commercial rechargeable batteries with high energy density can be made possible by substituting monovalent ions (Li^+, Na^+) with divalent Mg^{2+}ions [8].

However, realizing the excellent electrochemical performance of Mg metal batteries requires outstanding Mg electrolytes [9–11]. Previous research has shown that Mg metal can only be reversibly plating/stripping in electrolytes with ether-based solvents [12]. Aurbach et al. created the world's first RMBs prototype, which used $Mg(AlCl_2BuEt)_2$/THF as the electrolyte and Mo_6S_8 as the cathode material [13]. However, due to the limited electrochemical stabilization window of this electrolyte, there was still a lot of opportunity for advancement. Following this direction, Aurbach et al. further developed electrolytes such as APC (PhMgCl+$AlCl_3$/THF) [14], MACC ($MgCl_2$+$AlCl_3$/THF) [15], which accelerated the development of RMBs. In recent years, boron-based electrolytes have attracted the attention of researchers due to their weak corrosiveness to the collector and high oxidation stability [12]. Guo et al. [16]. created a boron-based magnesium electrolyte with boron as the anionic core atom with strong oxidation stability (3.5 V versus Mg), however, the complicated synthesis based on the format reaction makes large-scale use problematic. Ren et al. [17] created a boron-based magnesium electrolyte with boron as the anionic core atom ($B(OR^F)_4^-$) possessing high fluorinated bulky and weakly coordinated.

* Corresponding authors.
E-mail addresses: zhanglei1990@whut.edu.cn (L. Zhang), xiaoyuan2013@cqu.edu.cn (X. Zhou), anqinyou86@whut.edu.cn (Q. An).

https://doi.org/10.1016/j.ensm.2024.103679
Received 29 May 2024; Received in revised form 5 July 2024; Accepted 29 July 2024
Available online 30 July 2024

Subsequently, a series of boron-based electrolytes were born using $Mg(BH_4)_2$ [18], $Mg(CB_{11}H_{12})_2$ [19] and $Mg(B(hfip)_4)_2$ [20] as Mg salts. Among them, the electrolyte represented by $Mg(B(hfip)_4)_2$ has excellent oxidation stability, relatively low overpotential, and is effectively compatible with various types of cathode materials. However, the complicated synthesis and expensive raw materials make large-scale use problematic. In summary, designing low-cost, conveniently manufactured electrolytes with good electrochemical properties and high compatibility are ongoing quest for researchers [21].

Fortunately, the phenol-based magnesium electrolyte meets these requirements. Wang et al. proposed the first-generation phenol-based Mg electrolytes, in which $(BMPMC)_2$-$AlCl_3$/THF [22] has good electrochemical performance and excellent water and oxygen resistance, however, the extremely low oxidation stability (~2.6 V vs. Mg/Mg^{2+}) severely limits its application to the high-voltage cathode. The rational introduction of substituents is one of the effective methods to efficiently improve the electrochemical performance of electrolytes. In studies related to potassium-ion battery electrolytes, targeted methylation of phosphate ester molecules has been used to achieve a balance between ionic conductivity, oxidation stability, and solvation ability [23–25]. The phenolic structure is flexible in design due to its multiple active sites. Subsequent researchers have optimized the performance of electrolytes by changing the type of phenolic substituents. Emily G. Nelson et al. [26] revealed that electron-withdrawing group substitution can effectively improve the oxidation stability of magnesium phenoxy electrolytes to 3.05 V. However, it still does not meet the requirements for the application of high-voltage RMBs.

A large amount of work has been reported on fluorination to significantly enhance the oxidation stability of electrolytes in recent years [27,28], but little has been reported on the reasonable control of the degree of fluorination. While fluorination can significantly enhance the oxidation stability of an electrolyte, excessive fluorination can have several detrimental effects, such as significantly increasing the viscosity of the electrolyte or severely reducing the ionic conductivity of the electrolyte. Therefore, the rational design of the degree of fluoridation is essential. In addition, the benzene ring in the phenolic structure has many active sites, and it is important to rationally utilize the site properties to protect the active sites to achieve the high voltage performance of the electrolyte.

Herein, we used an electron-withdrawing group (-F) as the phenol substituent group and anchored the two fluorine groups to the 2,4 sites, respectively. The -F at the 2,4-sites stabilizes the ortho-site and para-site (o-para site) activated by O^-. Meanwhile, the electron-withdrawing fluorine groups significantly diminish the electron cloud density of phenol, (we christened as fluorine-based localization effect). Accordingly, we create a difluorinated phenol-based magnesium electrolyte (M24AT) with optimum oxidation stability. The phenol 2,4 active sites are substituted with two fluorine groups for better electronic delocalization and better resistance to electrophilic attack. This brings an oxidation stability up to 3.9 V vs. Mg/Mg^{2+} of the M24AT electrolyte. Meanwhile, the more fluorinated M24AT electrolyte can in-situ generate stable fluorinated SEI on the Mg anode. Based on these improvements, Mg || Mg symmetric cell with M24AT electrolyte can cycle for 900 h at a current density of 0.1 mA cm^{-2} and a low polarization of ~100 mV. In addition, the Mg||Cu half-cell has an average coulombic efficiency (CE) greater than 99.5 % in nearly 800 cycles. Furthermore, the Mg || Mo_6S_8 full cells retain ~100 % capacity retention (79.32 mAh g^{-1}) after 500 cycles at 1C (128.8 mA g^{-1}), demonstrating the potential of the M24AT electrolyte. To highlight even further the advantages of magnesium phenol electrolytes versus other chlorine-containing electrolytes, we assembled Mg||M24AT||Mo_6S_8 pouch cells in the air and exhibited more than 200 stable cycles. It is also compatible with the P14AQ and the PAQI high-voltage organic polymer cathode, which can be stably cycled 400 cycles at 5C (P14AQ), and a high-voltage discharge platform of ~1.8 V (PAQI). The present work refocuses the attention on magnesium phenol electrolytes, although the related research has been shelved for many years. This work proposes a new universal design principle for magnesium phenol electrolytes and accordingly obtains the M24AT electrolyte with a variety of excellent properties, realizing the first use of this type of electrolyte in high-voltage magnesium-metal batteries.

2. Results and discussion

Previously published research indicates that by substituting the phenol-based active sites with electron-withdrawing groups (such as trifluoromethyl (-CF_3) and fluorine (-F)), the electron cloud density of the phenol groups can be reduced, which effectively improves the oxidation stability of phenol-based Mg electrolytes (Fig. 1a, Fig S1). However, the electrolyte oxidation stability of single fluorine and single trifluoromethyl substituted phenol groups still falls short of expectations [26,29]. In this study, we proposed to increase the number of substituents to improve the oxidation stability of phenol-based magnesium electrolytes. Taking the difluorophenol as an example, ESP isosurface calculations for difluorophenols show that all difluorophenols have a more dispersed electron on the benzene ring and a much lower electron cloud density relative to phenol (Fig. 1b). Detailed steps (Fig. 1c) for the synthesis of phenol-based magnesium electrolytes can be found in the Supporting Information.

Unfortunately, the prepared electrolytes cannot reversibly Mg plating/stripping when the phenol structural site is replaced by two trifluoromethyl substituents (Fig. 1d, Fig. S2). In addition, when two trifluoromethyl groups are substituted for phenol, the conductivity of the electrolyte deteriorates sharply, and the viscosity increases significantly (Fig. S3). -CF_3 as a strong electron-withdrawing group, has a much higher electron-withdrawing capacity than fluorine groups, indicating that excessive electron-withdrawing group substitution does not result in an optimal phenol-based electrolyte (Fig. 1d). However when two fluorine groups replace two active sites of the phenol group, the oxidation stability of all the resulting electrolyte exceeds 3.5 V in Mg|| Mo cells (Fig. S4). In particular, the magnesium electrolyte configured with 24-difluorophenol achieved an oxidation stability of 3.9 V (Fig S4). This exceeds the level of all previously published phenol-based magnesium electrolytes. Equivalently, excessive -F substitution is clearly undesirable. The oxidation stability of the electrolyte prepared using pentafluoro phenol as the raw material was reduced to 3.05 V [26]. Additionally, The oxidation stability of the magnesium electrolyte configured with 246-trifluorophenol was reduced to 3.5 V (Tab. S1, Fig. S5). The oxidation stability of an electrolyte depends mainly on the least stable substance in it and is usually determined by unstable anions in magnesium-ion battery electrolytes [16]. Thus, the main reason for the reduced oxidation stability of the electrolyte compared to difluorophenol is the lower electron cloud density of pentafluoro phenol, which in turn leads to a weaker solvated ionic interaction with the aluminum ions, making the structure unstable. Based on a more comprehensive performance, we screened out difluorophenol as the preferred raw material for phenol-based Mg electrolytes.

Obviously, difluorophenol has a variety of isomers, and different structures of difluorophenol also exhibit different performance characteristics. This work aims to guide the design of difluorophenol-based magnesium electrolytes with optimal performance through substituent localization effects. Next, we selected four distinct configurations of difluorophenol (namely, 2,4-difluorophenol, 2,5-difluorophenol, 2,6-difluorophenol, and 3,5-difluorophenol) as the raw material and synthesized the corresponding magnesium electrolytes. They were designated as M24AT, M25AT, M26AT, and M35AT, respectively.

NMR (Nuclear Magnetic Resonance), FTIR (Fourier transform infrared spectroscope), and Raman spectroscope are practical approaches to define the composition of the electrolyte [8]. The ^{27}Al spectra can show the chemical environment of the aluminum ions. Compared to the ^{27}Al spectra of the $AlCl_3$/THF solution, the M24AT electrolyte presents four different chemical states of aluminum-solvated anions (Fig. 2a, Fig. S6). This corresponds to 52 ppm of Al([(2,

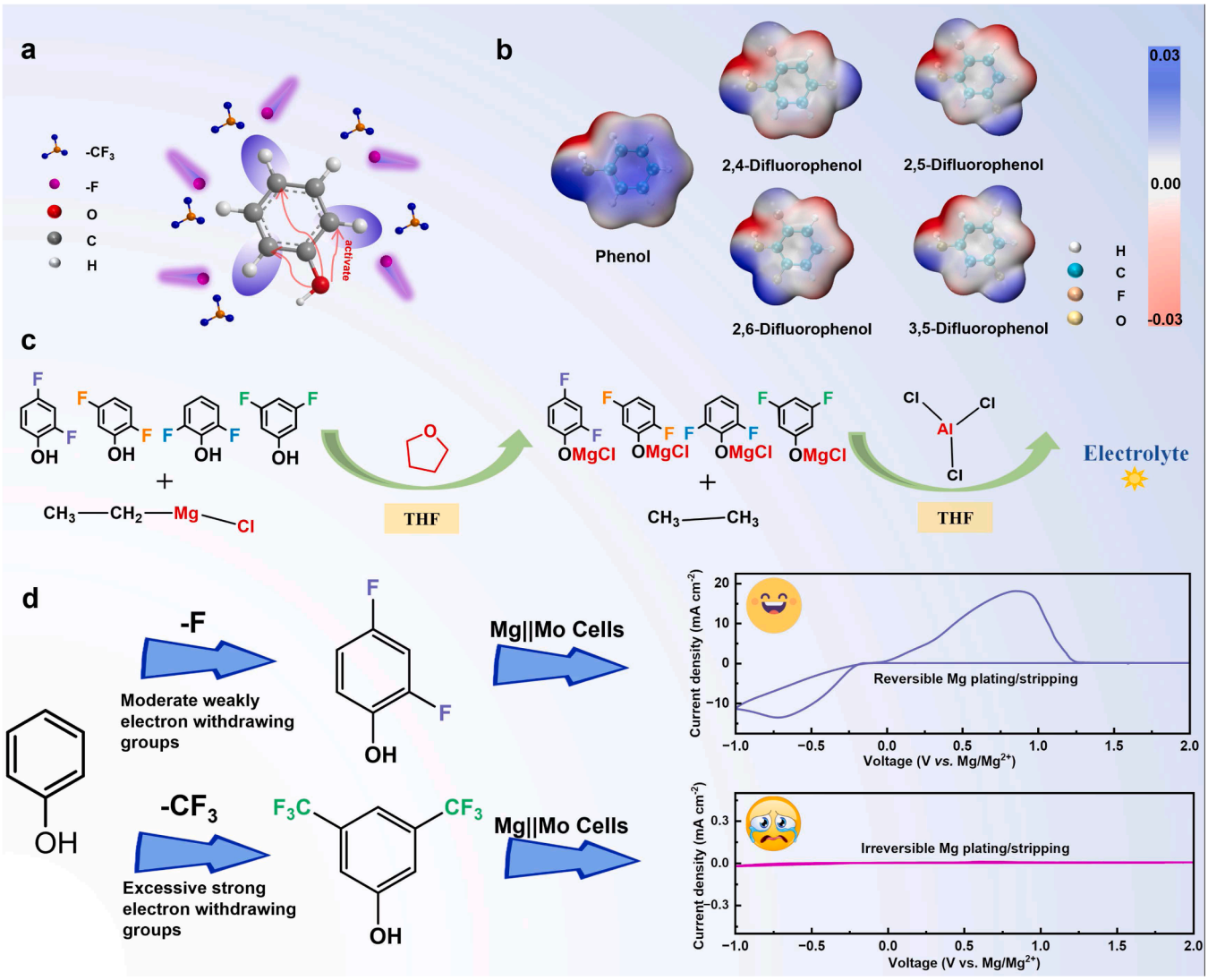

Fig. 1. (a) Ways to enhance the oxidation stability of phenol-based electrolytes. (b) Visualization of the DFT theoretical calculation. [30] ESP isosurface of Phenol, 2, 4-difluorophenol, 2,5-difluorophenol, 2,6-difluorophenol, 3,5-difluorophenol; the negative charge is represented in red and the positive is represented in blue. (c) Synthesis steps for the electrolytes of M24AT, M25AT, M26AT, and M35AT. (d) Phenol-based electrolyte design requires moderate substitution of electron-withdrawing groups. The CV curve of the electrolytes prepared from 3,5-bis (trifluoromethyl) phenol does not allow for reversible stripping/plating of magnesium.

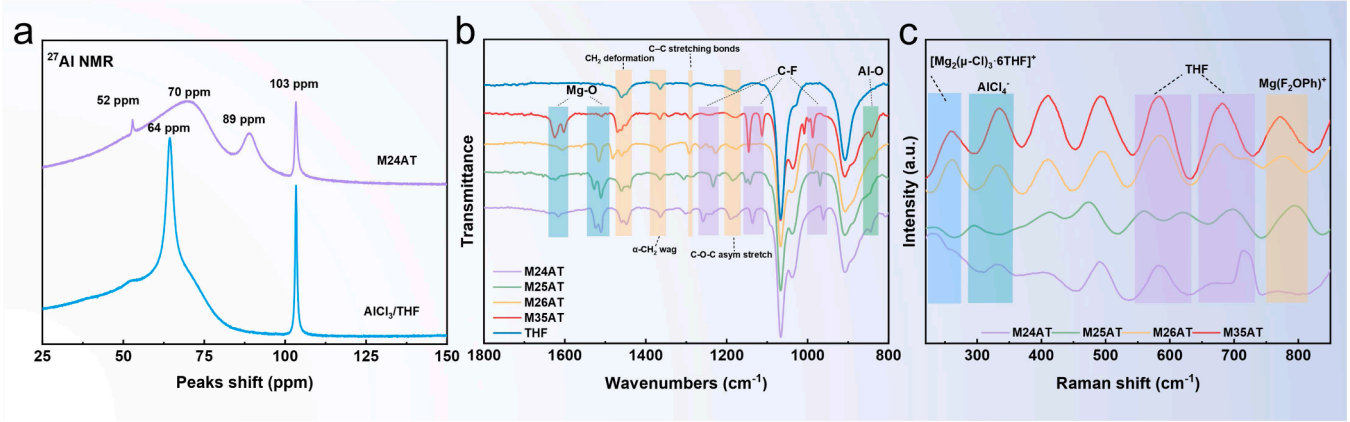

Fig. 2. (a) ^{27}Al NMR Spectra of M24AT and $AlCl_3$/THF Solutions. (b) FTIR spectrum of M24AT, M25AT, M26AT, M35AT, THF. (c) Raman spectroscopy of M24AT, M25AT, M26AT, M35AT.

4-F_2PhO)])$_4^-$, 70 ppm of AlCl([(2,4-F_2PhO)])$_3^-$, 89 ppm of $AlCl_2$([(2, 4-F_2PhO)])$_2^-$, and 103 ppm of Al_2Cl_6 in the 27Al spectral peak [26]. The presence of Al-O (near 1040cm^{-1}) in the FTIR also indicates the formation of polymorphs of Al anion with phenoxy ions (Fig. 2b) [31,32]. Meanwhile, the solvated structure of the aluminum anion can indicate the presence of reactive magnesium species. The Raman peaks located at near 260 cm^{-1} and 340 cm^{-1} clearly show the generation of $[Mg_2(\mu\text{-}Cl)_3\cdot 6THF]^+$ and $AlCl_4^-$ in the electrolyte (Fig. 2c) [33].

To compare the performance of electrolytes prepared from different structures of difluorophenol as raw materials, Mg||Mo half-cells were assembled, and the performance of the four electrolytes was tested by cyclic voltammetry (CV). The results showed that all electrolytes could plating/stripping magnesium reversibly (Fig. 3a, Fig. S7). As shown in the cyclic voltammogram (Fig. 3c), the M24AT electrolyte has a striping potential at −0.066 V and a plating potential at −0.147 V, giving an overpotential of 81 mV [34]. The M24AT electrolyte has the lowest overpotential of four electrolytes (Fig. 3d, Fig. S8). In the early stage of electrolyte cycles, there is a small amount of aluminum element deposition in the electrolyte (Fig. S9). As the CV cycle proceeds, the aluminum deposition behavior is gradually suppressed, showing a single deposition peak of magnesium. In addition, we analyzed the CV test results of the four electrolytes, plotted the trend of Q-Q_0 over time for the four electrolytes, and accordingly analyzed in detail the Coulombic efficiency changes in the first ten cycles. The results show that the Coulombic efficiencies of the four electrolytes increase dramatically over the five cycles After the sixth cycle, the Coulombic efficiency approaches 100 % (Fig. 3e, Fig. S10). This strongly indicates the excellent Mg plating/stripping efficiency of this type of electrolyte. Besides, the M24AT electrolyte has the highest response current under the same experimental conditions (Fig. 3a, Fig. S7). This indicates that the faster Mg redox kinetics in the M24AT electrolyte. To determine the oxidation stability of the four electrolytes, we performed linear scanning voltammetry (LSV) tests. As envisaged, the M24AT electrolyte had the strongest voltage tolerance (Fig. 3b). Its oxidation stability can reach 3.9 V (vs.

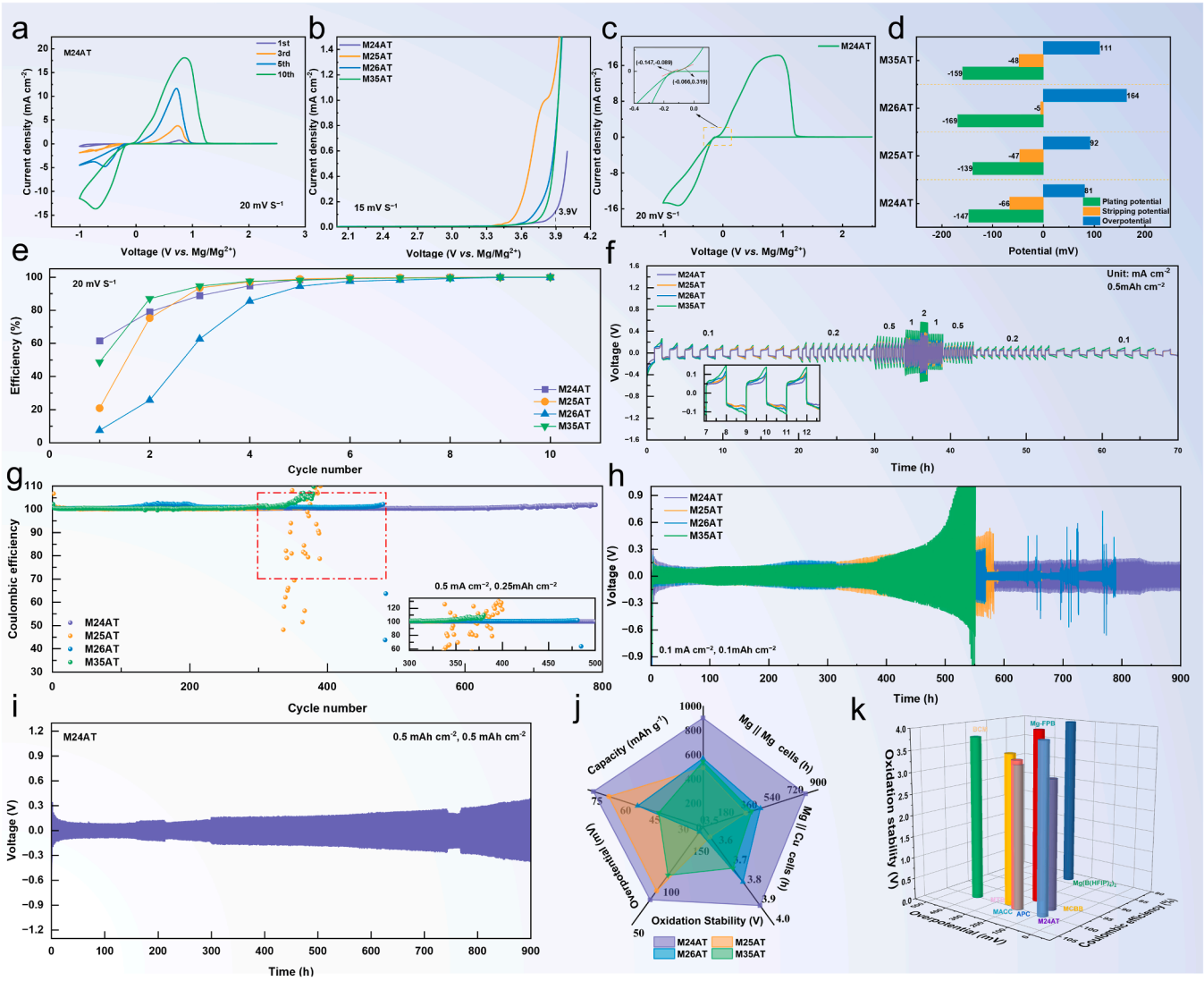

Fig. 3. Electrochemical performance. Cyclic voltammograms of the Mg plating and stripping process using (a) M24AT electrolyte. The CV was studied by a three-electrode system using Mg as the reference and counter electrode and Mo as the working electrode at a scanning rate of 20 mV S^{-1}. (b) Oxidation stability of four electrolytes in Mg || Mo half cells tested by LSV. (c) Mg plating/stripping overpotential in M24AT. Calculation of overpotential concerning Mg-FPB electrolyte. [34] (d) Comparison of overpotentials of four electrolytes. (e) Coulombic efficiency of different electrolytes obtained by cyclic voltammetry. (f) Polarization properties of Mg||Mg symmetrical cells with four electrolytes at current densities from 0.1 mA cm^{-2} to 2 mA cm^{-2}. (g) Mg plating/stripping CE in Mg || Cu half cells using four electrolytes at 0.5 mA cm^{-2} and 0.25 mAh cm^{-2}. Insets show an enlarged view of the cycles framed by the one dashed rectangle. (h) Rate performance of Mg||Mg cells at 0.1 mA cm^{-2} and 0.1 mAh cm^{-2}. (i) Polarization properties of Mg||Mg symmetrical cell with M24AT electrolyte at current density of 0.5 mA cm^{-2} and 0.5 mAh cm^{-2}. (j) Performance comparison of four electrolytes. (k) Performance comparison of the reported electrolytes with M24AT electrolyte.

Mg/Mg^{2+}). This means that the M24AT electrolyte can be matched to a high-voltage cathode.

Mg || Cu asymmetric cells were assembled to rate the coulombic efficiency of reversible Mg plating/stripping in all electrolytes at 0.5 mA cm^{-2} and 0.25 mAh cm^{-2} (Fig. 3g). It is obvious that M24AT has the most stable CEs with approaching 800 stable cycles. Excitingly, the average CE is close to 100 %. This highlights the fact that the M24AT electrolyte has the most superior Mg plating/stripping efficiency. Mg || Mg symmetric cells were assembled to evaluate the stability and compatibility of Mg anode in different electrolytes. Increasing the symmetric cell current density from 0.1 mA cm^{-2} to 2 mA cm^{-2} resulted in a gradual increase in the measured polarization (Fig. 3f). Among them, the M24AT electrolyte showed the smallest enhancement in polarization. Which also can reflect that M24AT has the best rate performance. In addition, these four electrolytes were subjected to long cycling tests at a current density of 0.1 mA cm^{-2}, and the M24AT electrolyte retained minimal polarization (~100 mV) for more than 900 h (Fig. 3h). Furthermore, the M24AT electrolyte present low polarization (Fig. 3i) at higher current density (0.5 mAh cm^{-2}, 0.5 mAh cm^{-2}). That is a prerequisite for the subsequent long cycling tests of the electrolyte with matched cathode materials.

The M24AT electrolyte has a better long-cycle performance, which may also be related to the magnesium deposition morphology. This stems from the fact that the smooth and dense magnesium deposition structure formed during electrolyte cycling is less likely to puncture the diaphragm and cause a short circuit in the battery, contributing to the battery's long-cycle performance. We analyzed the morphology of the deposited magnesium formed during the discharge of all electrolytes by scanning electron microscopy (SEM) through a three-electrode system. The results indicate that deposited magnesium obtained from M24AT with the smoothest and densest state (Fig. S9, Fig. S11, Fig S12).

According to the rules of orientation effect of electrophilic aromatic directing groups, phenoxy (O-) mainly activates the ortho-site and para-site (o-para site) of the benzene ring. However, since the o-para site is occupied by a fluorine group, the activation site is not susceptible to electrophilic attack, and the fluorine group acts as an electron-withdrawing group to significantly reduce the electron cloud density of the benzene ring to stabilize the structure (we define this principle called fluorine-based localization effect). All of the above raw materials of electrolytes are difluorophenols, but the substitution sites are different. According to the orientation effect of electrophilic aromatic directing groups, activating the benzene ring at the o-para site (2,4,6 site) makes it vulnerable to electrophilic assault. Due to the fluorine substitution occupying the o-para site, 2,4-difluorophenol and 2,6-difluorophenol have good electrolyte stability. However, 2,6-difluorophenol is less stable than 2,4-difluorophenol because the latter has a lower electron cloud dispersion. Due to the occupation of fewer o-para sites, 3,5-difluorophenol and 2,5-difluorophenol are lower stable in the structure of the respective electrolytes. But the 3,5-sites substitutions raise space substituted steric hindrance of other sites and make M35AT more stable than M25AT. As a result, the four electrolytes are ranked according to the magnitude of their oxidation stability: M24AT > M26AT > M35AT > M25AT (Fig. 3b). It is the difference in the substitution site of the fluorine groups that renders the difference in the properties of different difluorophenols.

The 2,4 active site fluorine-substituted difluorophenol-based magnesium electrolyte possesses the best performance due to the fluorine-based localization effect. (Fig. 3j). This will provide theoretical support for the design of high-performance phenol-based magnesium electrolytes.

Besides, the highest oxidation stability and a more dispersed electron cloud density of 2,4-difluorophenol are intriguing to notice because they improve the separation of magnesium chloride ions ($MgCl^+$) from the intermediate 2,4-difluorophenol magnesium chloride (2,4-F_2PhOMgCl). The M24AT electrolyte will have the greatest electrochemical performance as a result (Fig. 3k, Tab S2).

The oxidation stability, ionic conductivity, the solvent ion coordination state of the electrolyte, and SEI can directly affect the electrochemical performance of magnesium batteries [17,28,35]. Among of them, SEI layer instability is a key barrier to long-cycle performance in RMBs [28,36,37]. Mai et al. demonstrated that fluorine-containing organic-inorganic hybrid SEIs can significantly enhance the long-cycle performance of magnesium batteries [31]. Consequently, we expect to rationally adjust the elemental composition of the electrolyte components on the basis of improving the oxidation stability of the electrolyte to regulate the SEI interface so that it can be better matched with the high-voltage cathode. Fortunately, the elemental fluorine in the M24AT electrolyte is expected to generate a stable fluorine-containing SEI.

DFT calculations for the four electrolytes confirm that M24AT has the lowest LUMO orbital energy (Fig. 4a). This means that M24AT is more readily decomposed at the magnesium anode to generate stable fluorinated SEIs.

To demonstrate the positive effect of the SEI formed after cycling of the M24AT electrolyte on overpotential and coulombic efficiency. We assembled Mg||Mg symmetric cells using M24AT as the electrolyte. The cell was cycled for 50 times to allow sufficient formation of a stable SEI. Subsequently, the cell was disassembled in a glove box and the electrode were removed to be cleaned and dried for use. A symmetric cell with magnesium electrodes containing fluorinated SEI was assembled using $Mg(TFSI)_2$/DME as the electrolyte. A magnesium symmetric cell with brand-new magnesium electrodes was also assembled as a control group. It was found that the polarization of the symmetric cell was greatly reduced compared with that of the control group due to the presence of the fluorinated interface generated by M24AT (Fig. 4c).

To gain insight into the structure of SEIs and interfacial mechanisms. We selected characterization such as X-ray photoelectron spectroscopy (XPS) and time-of-flight secondary-ion mass spectrometry (TOF-SIMS) to analyze the composition of SEI from the surface to the interior. For the Mg anode cycled in M24AT electrolyte, the Mg-F (685.4 eV) peak gradually dominates with increasing SEI depth (Fig. 4d). This indicates a longitudinal massive distribution of Mg_xF originating from the decomposition of electrolyte components. The cells were disassembled and the XPS testing of the Mg anode was carried out in a glove box without water or oxygen. However, the peak of the oxide (529.5 eV) gradually dominates (Fig. 4d), indicating that the SEI contains a Mg_xO_y/Al_xO_y component. It again stems from the decomposition of the electrolyte component. We also used the time-of-flight secondary-ion mass spectrometry (TOF-SIMS) to analyze the composition and longitudinal distribution of SEI in the post-cycling Mg anode (Fig. 4e-h). The large distribution of fluoride-containing ions (F^-, MgF^+) and organic fragment ions (CHO_2^+, CH^-) suggests that the M24AT electrolyte can generate stable fluorinated organic-inorganic hybrid SEIs during cycling. This may contribute to the long cycling process of the battery. It is also possible that the high oxidation stability of M24AT stems from the stabilization of the electrolyte composition by fluorinated SEI in situ generated during electrolyte cycling.

The utility of the electrolyte can be reflected by the degree of compatibility between the electrolyte and the cathode material. To evaluate the compatibility of electrolytes with cathode materials, we assembled Mg||Mo_6S_8 full cells. The cathode material Mo_6S_8 was used to confirm the successful synthesis by X-ray diffraction spectroscopy (XRD) (Fig. S13).

The CVs of the Mg||Mo_6S_8 cells reflect the lowest polarization and strongest response current of the M24AT electrolyte (Fig. 5a), which suggests that the inserting/extracting of Mg^{2+} in the cathode is prioritized. In addition, M24AT also showed the best rate performance (Fig. 5c), with no large loss of capacity of the Mo_6S_8 cathode material at different rates (from 0.5 C to 5 C). Specifically, from the charge/discharge curves of M24AT, it can be seen that the polarization of the cell stays low at high rates of charge/discharge (Fig. 5b). M24AT electrolyte maintains the highest charge/discharge specific capacity compared to other electrolytes under the 0.5C long cycle test (Fig. 5d).

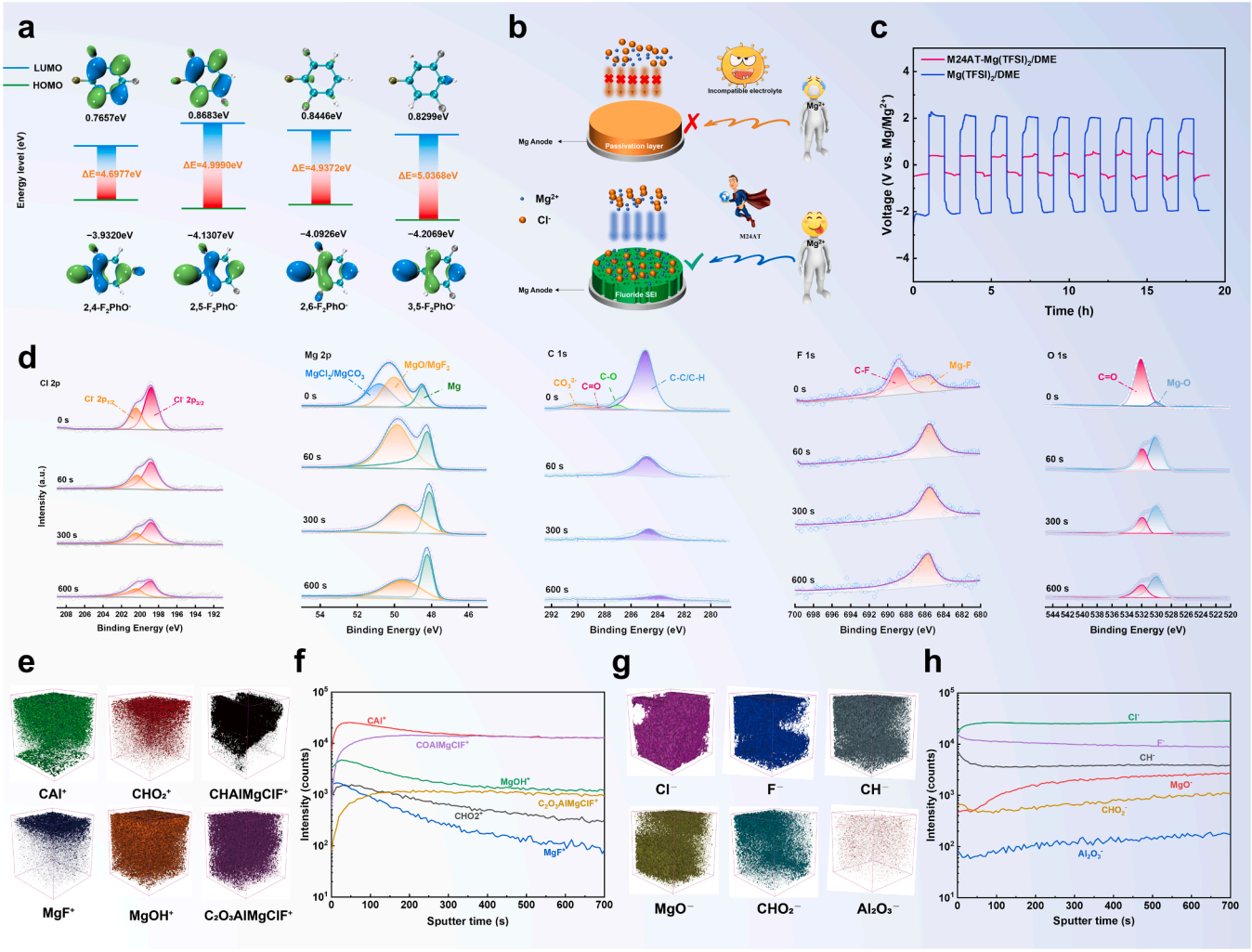

Fig. 4. (a) Visualization of the DFT theoretical calculation. Visualized LUMO/HOMO orbitals and transition gap energy of 2,4-difluorophenoxy ($[(2,4\text{-}F_2PhO)]^-$), 2,5-difluorophenoxy ($[(2,5\text{-}F_2PhO)]^-$), 2,6-difluorophenoxy ($[(2,6\text{-}F_2PhO)]^-$), 3,5-difluorophenoxy ($[(3,5\text{-}F_2PhO)]^-$) anions. (b) Schematic representation of the M24AT electrolyte for the generation of a stable fluorinated SEI in a magnesium metal cell. (c) The fluorinated SEI generated by the M24AT electrolyte effectively reduces cell polarization. (d) F 1 s, O 1 s, Mg 2p, Al 2p XPS depth analysis of Mg anode. 3D rendering and TOF-SIMS depth profiles models in (e, f) positive mode and (g, h) negative mode of the SEI film cycled with the M24AT electrolyte.

Under the 1C long cycling test, M24AT electrolyte still has a high specific capacity of 79 mAh g^{-1} after 500 cycles (capacity retention of ~100 %), which is better than most of the reported electrolytes (Fig. 5e).

The realization strategy of high-energy magnesium-metal batteries requires cathode materials to have higher theoretical specific capacity on the one hand, and magnesium-metal batteries to be able to operate at higher voltages on the other hand [11]. The latter requires more electrolytes with better high-voltage stability and compatibility.

Generally speaking, compared with the traditional inorganic cathode materials, the new organic cathode materials have higher discharge platforms and higher operating voltages. Herein, polyanthraquinonylimides (PAQI) were synthesized and investigated as organic RMB cathodes. Surprisingly, when the Mg||PAQI full cell was assembled using the M24AT electrolyte, the discharge plateau voltage was as high as 1.8 V (Fig. 5f and Fig. 5g). This value is a significant improvement over the first published discharge plateau voltage for electrochemical testing of PAQI cathode materials, which was 1.6 V [38]. Furthermore, after we increased the voltage test range and set the upper voltage limit to 3.0 V, the battery still operated stably. Specifically, the Mg||PAQI full cell can be stably cycled more than 300 cycles at a current density of 200 mA g^{-1}. This realizes the first use of magnesium phenol electrolyte in high-voltage magnesium metal batteries.

The M24AT electrolyte also has good compatibility with high-voltage organic cathode materials (PAQI). The assembled Mg||P14AQ full cells have a specific capacity of 87.72 mAh g^{-1} (capacity retention of 72.8 %) after cycling over 200 cycles at 2C (Fig. 5h-i). Specific capacity of 69.78 mAh g^{-1} (capacity retention of 68.7 %) after over 400 cycles at 5C (Fig. 5h-i). In addition, we assembled a Mg||Mo_6S_8 pouch cell to light up the lamp (Fig 6a). Various results show that the M24AT electrolyte has great potential for matching cathode materials.

Magnesium phenol electrolyte has good ionic conductivity, lower raw material cost and better compatibility with cathode materials. To highlight even further the advantages of magnesium phenol electrolytes versus other chlorine-containing electrolytes, we conducted a water-oxygen tolerance test on the M24AT electrolyte. After exposing the M24AT electrolyte to humid air for 3 h, the Mg||M24AT||Mo cell was assembled for cyclic voltammetry testing. Unlike the results of previous work testing the APC electrolyte's resistance to hydroxylation, the cyclic voltammetry curves of the M24AT electrolyte show that it is still capable of plating/stripping magnesium metal stably. The results show that M24AT has excellent water-oxygen tolerance compared with APC electrolytes (Fig. 6b, Fig. S14). In addition, to highlight the advantages of the M24AT electrolyte even further, we assembled the magnesium metal pouch cell entirely in the air. Excitingly, the newly assembled

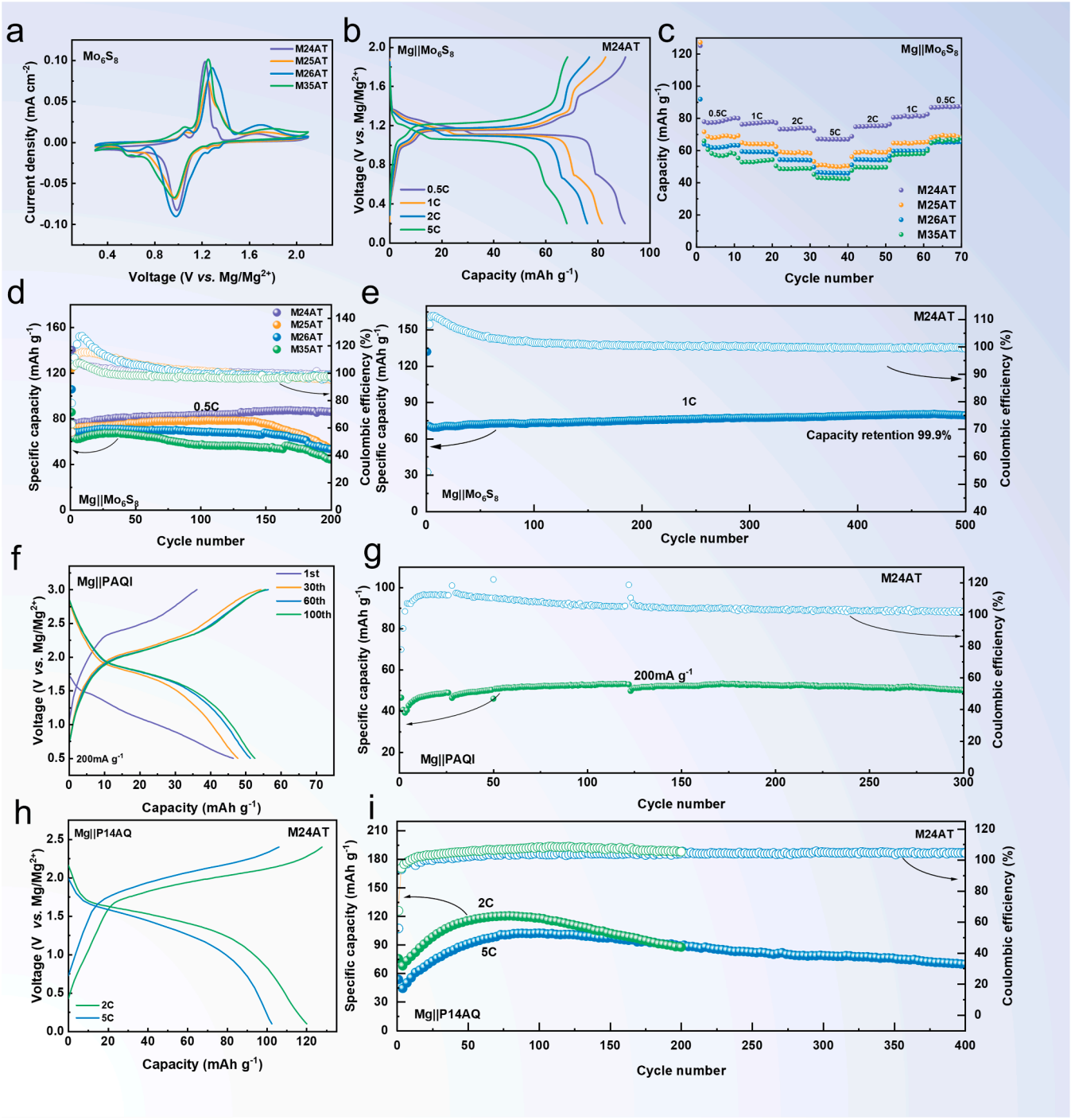

Fig. 5. Mg || Mo_6S_8 full cell performance in different electrolytes. (a) Cyclic voltammograms with a scan rate of 0.1 mV s^{-1}. (b) Charge/discharge profile with a voltage range of 0.2 − 1.9 V (vs. Mg/Mg^{2+}) in M24AT electrolyte at various current densities. (c) Rate performance at various current densities from 0.5 to 5 C. (d) Cycling performance over 200 cycles at 0.5 C (1 C = 128.8 mA g^{-1}). (e) Long-term cycling performance at 1 C. (f) Charge/discharge profile of Mg || PAQI full cells with M24AT electrolyte at 200mA g^{-1} . (g) Cycling performance. Mg || P14AQ full cell performance in M24AT electrolyte. (h) Charge/discharge profile of Mg || P14AQ full cell with M24AT electrolyte at 2 C and 5 C. (i) Cycling performance over 200 cycles at 2 C (1 C = 260 mA g^{-1}) and over 400 cycles at 5C.

Mg||Mo_6S_8 has an open-circuit voltage of up to 2.14 V and can be stably cycled for more than 200 cycles at a multiplication rate of 2C (Fig. 6c and Fig. 6d).

The above results indicate that the utilization of fluorine-based localization effects can be used as a general strategy for the preparation of magnesium phenol electrolytes. Inexpensive, high ionic conductivity, M24AT electrolytes that can generate excellent fluorinated interfaces, high voltage stability, and strong water-oxygen resistance can be obtained.

3. Conclusion

In summary, this work focuses on phenol-based magnesium electrolytes from a novel perspective, and the design of a difluorides-substituted phenol-based magnesium electrolyte with optimal performance by anchors the 2,4 sites via a weakly electron-withdrawing group (-F). Furthermore, the significantly improved oxidation stability of the M24AT electrolyte compared to all other phenol-based magnesium electrolytes has led to the first application of this type of electrolyte in

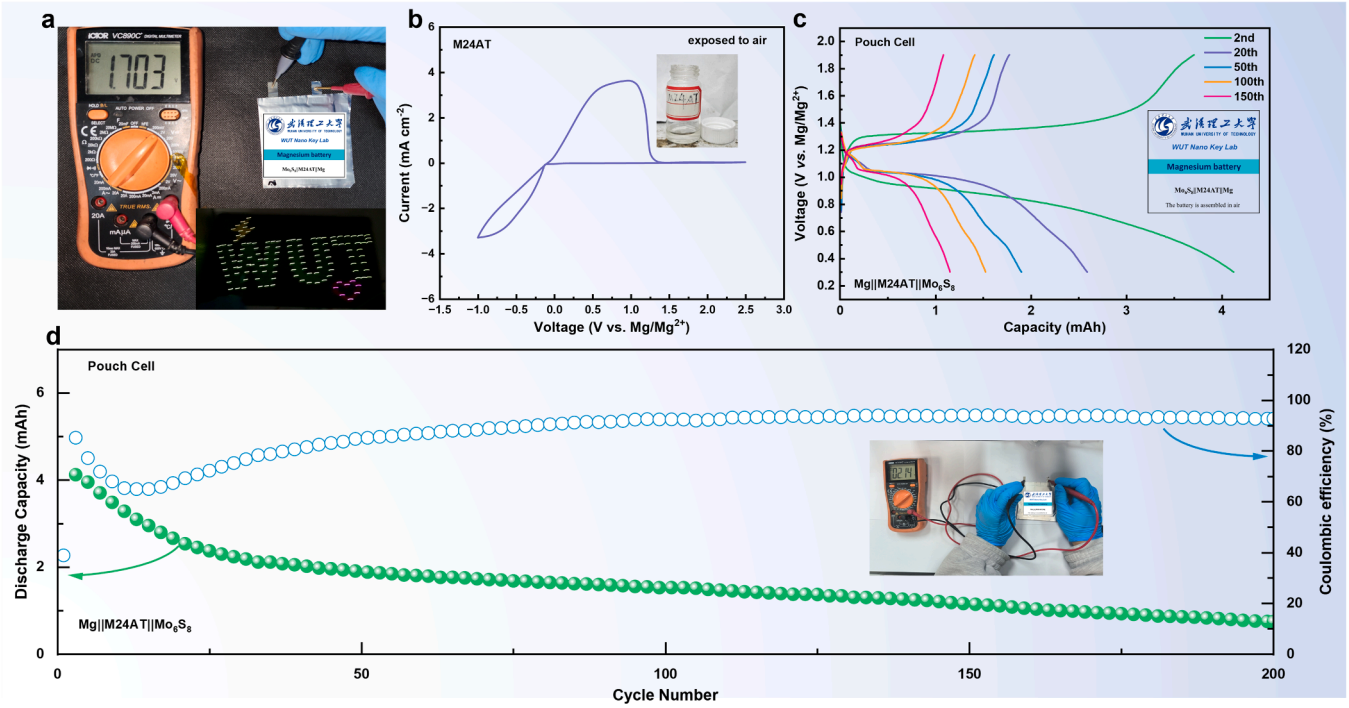

Fig. 6. (a) Mg || Mo_6S_8 Pouch cell with M24AT electrolyte. Water-oxygen resistance test of M24AT electrolyte (b) Cyclic voltammograms of M24AT electrolyte exposed to air for 3 h with a scan rate of 20 mV s^{-1}. (c-d) Electrochemical performances of Mg ||M24AT|| Mo_6S_8 pouch cell (was assembled at air) at 2C.

high-voltage magnesium-metal batteries. The M24AT electrolyte designed possessing the fluorine-based localization effect has optimal oxidation stability (3.9 V vs. Mg/Mg^{2+}) and the electrolyte can in situ generate fluorinated organic-inorganic hybrid SEI layers during the cycling process. Mg||Mo_6S_8 full cells assembled with M24AT electrolyte have a high capacity of 79.32 mAh g^{-1} after 500 cycles at 1C (capacity retention of ~100 %). In addition, the M24AT electrolyte also retains many of the advantages of the magnesium phenol electrolyte at the same time. Such as excellent resistance to water and oxygen, high ionic conductivity and very low raw material costs. The M24AT electrolyte remains electrochemically active when exposed to humid air. Mg||Mo_6S_8 pouch battery assembled in the air can maintain a long-term stable cycle, which also reduces the difficulty of production for the large-scale application of this type of electrolyte. Benefit from the fluorine-based localization effect of the M24AT electrolyte. The M24AT electrolyte also shows better compatibility, as-prepared Mg||P14AQ full cells have high-capacity retention after 400 cycles at 5C. Besides, the assembled Mg||PAQI cell operates at voltages up to 3.0 V and exhibits a high voltage discharge platform of ~1.8 V. We believe this work provides new insights into present and future electrolyte design and can advance the process of high-voltage RMBs practicality.

CRediT authorship contribution statement

Pei Liu: Writing – original draft, Visualization, Investigation, Formal analysis, Conceptualization, Data curation, Methodology, Validation, Writing – review & editing. **Juncai Long:** Writing – review & editing, Conceptualization, Data curation, Formal analysis. **Rui Wang:** Data curation, Formal analysis, Investigation. **Yuhao Zhou:** Investigation, Data curation, Methodology. **Baihua Qu:** Data curation, Investigation, Writing – review & editing. **Lei Zhang:** Supervision, Data curation, Formal analysis, Writing – review & editing. **Xiaoyuan Zhou:** Data curation, Formal analysis, Methodology, Writing – review & editing. **Qinyou An:** Supervision, Funding acquisition, Conceptualization, Project administration, Writing – review & editing.

Declaration of competing interest

The authors declare that they have no known competing financial interests or personal relationships that could have appeared to influence the work reported in this paper.

Acknowledgements

Pei Liu, Juncai Long contributed equally to this work. This work was supported by the National Key Research and Development Program of China (No. 2023YFB3809501), the National Natural Science Foundation of China (52172231), the Natural Science Foundation of Hubei Province (2022CFA087), the Fundamental Research Funds for the Central Universities (WUT: 2023-vb-004).

Supplementary materials

Supplementary material associated with this article can be found, in the online version, at doi:10.1016/j.ensm.2024.103679.

References

[1] H.D. Yoo, E. Markevich, G. Salitra, D. Sharon, D. Aurbach, On the challenge of developing advanced technologies for electrochemical energy storage and conversion, Mater. Today 17 (2014) 110–121, https://doi.org/10.1016/j.mattod.2014.02.014.
[2] A. Manthiram, Correction to "materials challenges and opportunities of lithium ion batteries, J. Phys. Chem. Lett. 2 (2011) 373, https://doi.org/10.1021/jz2001216.
[3] D. Lin, Y. Liu, Y. Cui, Reviving the lithium metal anode for high-energy batteries, Nature Nanotech 12 (2017) 194–206, https://doi.org/10.1038/nnano.2017.16.
[4] X. Zhang, Y. Yang, Z. Zhou, Towards practical lithium-metal anodes, Chem. Soc. Rev. 49 (2020) 3040–3071, https://doi.org/10.1039/C9CS00838A.
[5] X. Zheng, L. Huang, X. Ye, J. Zhang, F. Min, W. Luo, Y. Huang, Critical effects of electrolyte recipes for li and na metal batteries, Chem 7 (2021) 2312–2346, https://doi.org/10.1016/j.chempr.2021.02.025.
[6] H. Zhang, L. Qiao, M. Armand, Organic electrolyte design for rechargeable batteries: from lithium to magnesium, Angew. Chem. Int. Ed. 61 (2022) e202214054, https://doi.org/10.1002/anie.202214054.
[7] H. Zhang, L. Qiao, H. Kühnle, E. Figgemeier, M. Armand, G.G. Eshetu, From lithium to emerging mono- and multivalent-cation-based rechargeable batteries: non-

aqueous organic electrolyte and interphase perspectives, Energy Environ. Sci. 16 (2023) 11–52, https://doi.org/10.1039/D2EE02998G.
[8] D. Zhang, S. Duan, X. Liu, Y. Yang, Y. Zhang, W. Ren, S. Zhang, M. Cheng, W. Yang, J. Wang, Y. NuLi, Deeping insight of mg(CF3SO3)2 and comprehensive modified electrolyte with ionic liquid enabling high-performance magnesium batteries, Nano Energy 109 (2023) 108257, https://doi.org/10.1016/j.nanoen.2023.108257.
[9] D. Zhang, Y. Wang, Y. Yang, Y. Zhang, Y. Zhao, M. Pan, Y. Sun, S. Chen, X. Liu, J. Wang, Y. NuLi, Constructing efficient mg(CF3SO3)2 electrolyte via tailoring solvation and interface chemistry for high-performance rechargeable magnesium batteries, Adv. Energy Mater. 13 (2023) 2301795, https://doi.org/10.1002/aenm.202301795.
[10] Y. Du, Y. Chen, S. Tan, J. Chen, X. Huang, L. Cui, J. Long, Z. Wang, X. Yao, B. Shang, G. Huang, X. Zhou, L. Li, J. Wang, F. Pan, Strong solvent coordination effect inducing gradient solid-electrolyte-interphase formation for highly efficient mg plating/stripping, Energy Storage Materials 62 (2023) 102939, https://doi.org/10.1016/j.ensm.2023.102939.
[11] H. Dong, O. Tutusaus, Y. Liang, Y. Zhang, Z. Lebens-Higgins, W. Yang, R. Mohtadi, Y. Yao, High-power mg batteries enabled by heterogeneous enolization redox chemistry and weakly coordinating electrolytes, Nat. Energy 5 (2020) 1043–1050, https://doi.org/10.1038/s41560-020-00734-0.
[12] R. Attias, M. Salama, B. Hirsch, Y. Goffer, D. Aurbach, Anode-electrolyte interfaces in secondary magnesium batteries, Joule 3 (2019) 27–52, https://doi.org/10.1016/j.joule.2018.10.028.
[13] D. Aurbach, Z. Lu, A. Schechter, Y. Gofer, H. Gizbar, R. Turgeman, Y. Cohen, M. Moshkovich, E. Levi, Prototype systems for rechargeable magnesium batteries, Nature 407 (2000) 724–727, https://doi.org/10.1038/35037553.
[14] O. Mizrahi, N. Amir, E. Pollak, O. Chusid, V. Marks, H. Gottlieb, L. Larush, E. Zinigrad, D. Aurbach, Electrolyte solutions with a wide electrochemical window for rechargeable magnesium batteries, J. Electrochem Soc. 155 (2008) A103, https://doi.org/10.1149/1.2806175.
[15] R.E. Doe, R. Han, J. Hwang, A.J. Gmitter, I. Shterenberg, H.D. Yoo, N. Pour, D. Aurbach, Novel, electrolyte solutions comprising fully inorganic salts with high anodic stability for rechargeable magnesium batteries, Chem. Commun. 50 (2013) 243–245, https://doi.org/10.1039/C3CC47896C.
[16] Y. Guo, F. Zhang, J. Yang, F. Wang, Y. NuLi, S. Hirano, Boron-based electrolyte solutions with wide electrochemical windows for rechargeable magnesium batteries, Energy Environ. Sci. 5 (2012) 9100, https://doi.org/10.1039/C2EE22509C.
[17] W. Ren, D. Wu, Y. NuLi, D. Zhang, Y. Yang, Y. Wang, J. Yang, J. Wang, An efficient bulky mg[B(otfe) $_4$] $_2$ electrolyte and its derivatively general design strategy for rechargeable magnesium batteries, ACS Energy Lett 6 (2021) 3212–3220, https://doi.org/10.1021/acsenergylett.1c01411.
[18] R. Mohtadi, M. Matsui, T.S. Arthur, S.-J. Hwang, Magnesium borohydride: from hydrogen storage to magnesium battery, Angew. Chem. Int. Ed. 51 (2012) 9780–9783, https://doi.org/10.1002/anie.201204913.
[19] O. Tutusaus, R. Mohtadi, T.S. Arthur, F. Mizuno, E.G. Nelson, Y.V. Sevryugina, An efficient halogen-free electrolyte for use in rechargeable magnesium batteries, Angew. Chem. Int. Ed. 54 (2015) 7900–7904, https://doi.org/10.1002/anie.201412202.
[20] Z. Zhao-Karger, R. Liu, W. Dai, Z. Li, T. Diemant, B.P. Vinayan, C. Bonatto Minella, X. Yu, A. Manthiram, R.J. Behm, M. Ruben, M. Fichtner, Toward highly reversible magnesium–sulfur batteries with efficient and practical mg[B(hfip)4]2 electrolyte, ACS Energy Lett 3 (2018) 2005–2013, https://doi.org/10.1021/acsenergylett.8b01061.
[21] R. Mohtadi, O. Tutusaus, T.S. Arthur, Z. Zhao-Karger, M. Fichtner, The metamorphosis of rechargeable magnesium batteries, Joule 5 (2021) 581–617, https://doi.org/10.1016/j.joule.2020.12.021.
[22] F. Wang, Y. Guo, J. Yang, Y. Nuli, S. Hirano, A novel electrolyte system without a grignard reagent for rechargeable magnesium batteries, Chem. Commun 48 (2012) 10763–10765, https://doi.org/10.1039/C2CC35857C.
[23] Y. Geng, H. Fu, Y. Hu, A.M. Rao, L. Fan, J. Zhou, B. Lu, Molecular-level design for a phosphate-based electrolyte for stable potassium-ion batteries, Appl. Phys. Lett. 124 (2024) 063901, https://doi.org/10.1063/5.0178871.
[24] Y. Hu, H. Fu, Y. Geng, X. Yang, L. Fan, J. Zhou, B. Lu, Chloro-functionalized ether-based electrolyte for high-voltage and stable potassium-ion batteries, Angew. Chem. Int. Ed. 63 (2024) e202403269, https://doi.org/10.1002/anie.202403269.
[25] L. Fan, H. Xie, Y. Hu, Z. Caixiang, A.M. Rao, J. Zhou, B. Lu, A tailored electrolyte for safe and durable potassium ion batteries, Energy Environ. Sci. 16 (2023) 305–315, https://doi.org/10.1039/D2EE03294E.
[26] E.G. Nelson, J.W. Kampf, B.M. Bartlett, Enhanced oxidative stability of non-grignard magnesium electrolytes through ligand modification, Chem. Commun. 50 (2014) 5193–5195, https://doi.org/10.1039/C3CC47277A.
[27] Y. Lin, Z. Yu, W. Yu, S.-L. Liao, E. Zhang, X. Guo, Z. Huang, Y. Chen, J. Qin, Y. Cui, Z. Bao, Impact of the fluorination degree of ether-based electrolyte solvents on li-metal battery performance, J. Mater. Chem.a 12 (2024) 2986–2993, https://doi.org/10.1039/D3TA05535C.
[28] J. Xiao, X. Zhang, H. Fan, Y. Zhao, Y. Su, H. Liu, X. Li, Y. Su, H. Yuan, T. Pan, Q. Lin, L. Pan, Y. Zhang, Stable solid electrolyte interphase in situ formed on magnesium-metal anode by using a perfluorinated alkoxide-based all-magnesium salt electrolyte, Adv. Mater. 34 (2022) 2203783, https://doi.org/10.1002/adma.202203783.
[29] B. Pan, J. Zhang, J. Huang, J.T. Vaughey, L. Zhang, S.-D. Han, A.K. Burrell, Z. Zhang, C. Liao, A lewis acid-free and phenolate-based magnesium electrolyte for rechargeable magnesium batteries, Chem. Commun. 51 (2015) 6214–6217, https://doi.org/10.1039/C5CC01225B.
[30] T. Lu, F. Chen, Multiwfn: a multifunctional wavefunction analyzer, J. Comput. Chem. 33 (2012) 580–592, https://doi.org/10.1002/jcc.22885.
[31] J. Long, S. Tan, J. Wang, F. Xiong, L. Cui, Q. An, L. Mai, Revealing the interfacial chemistry of fluoride alkyl magnesium salts in magnesium metal batteries, Angew. Chem. Int. Ed. 62 (2023) e202301934, https://doi.org/10.1002/anie.202301934.
[32] K.-C. Lau, T.J. Seguin, E.V. Carino, N.T. Hahn, J.G. Connell, B.J. Ingram, K. A. Persson, K.R. Zavadil, C. Liao, Widening electrochemical window of mg salt by weakly coordinating perfluoroalkoxyaluminate anion for mg battery electrolyte, J. Electrochem. Soc. 166 (2019) A1510, https://doi.org/10.1149/2.0751908jes.
[33] K.A. See, Y.-M. Liu, Y. Ha, C.J. Barile, A.A. Gewirth, Effect of concentration on the electrochemistry and speciation of the magnesium aluminum chloride complex electrolyte solution, ACS Appl. Mater. Interfaces 9 (2017) 35729–35739, https://doi.org/10.1021/acsami.7b08088.
[34] J. Luo, Y. Bi, L. Zhang, X. Zhang, T.L. Liu, A stable, non-corrosive perfluorinated pinacolatoborate mg electrolyte for rechargeable mg batteries, Angew. Chem. Int. Ed. 58 (2019) 6967–6971, https://doi.org/10.1002/anie.201902009.
[35] W. Zhao, Z. Pan, Y. Zhang, Y. Liu, H. Dou, Y. Shi, Z. Zuo, B. Zhang, J. Chen, X. Zhao, X. Yang, Tailoring coordination in conventional ether-based electrolytes for reversible magnesium-metal anodes, Angew. Chem. Int. Ed. 61 (2022) e202205187, https://doi.org/10.1002/anie.202205187.
[36] C. Li, A. Shyamsunder, B. Key, Z. Yu, L.F. Nazar, Stabilizing magnesium plating by a low-cost inorganic surface membrane for high-voltage and high-power mg batteries, Joule 7 (2023) 2798–2813, https://doi.org/10.1016/j.joule.2023.10.012.
[37] C.S. Santos, M. Romio, Y. Surace, N. Eshraghi, M. Amores, A. Mautner, C. Groher, M. Jahn, E. Ventosa, W. Schuhmann, Unveiling the electronic properties of native solid electrolyte interphase layers on mg metal electrodes using local electrochemistry, Chem. Sci. 14 (2023) 9923–9932, https://doi.org/10.1039/D3SC02840B.
[38] Y. Ding, D. Chen, X. Ren, Y. Cao, F. Xu, Organic-conjugated polyanthraquinonylimide cathodes for rechargeable magnesium batteries, J. Mater. Chem.a 10 (2022) 14111–14120, https://doi.org/10.1039/D2TA02795J.